Seismic bearing capacity of circular foundations

C. T. Chatzigogos, A. Pecker, J. Salençon

Solid Mechanics Laboratory, CNRS UMR 7649,
Department of Mechanics - Ecole Polytechnique, 91128 Palaiseau, France

Abstract

For the determination of the seismic bearing capacity of circular footings resting on the surface of a homogeneous purely cohesive isotropic half space, we extend the concept of "macro-element", which was introduced by Cremer, Pecker & Davenne (2001, 2002) for the treatment of dynamic soil-structure interaction analyses, to 3D configurations. The footing configurations under consideration are defined by six loading parameters, namely: the inclined force (N, V) and the moment (M) both acting at the center of the footing, a surcharge at the soil surface (q) and vertical and horizontal soil body forces (γ, f_h) accounting for the soil unit weight and for the inertial forces exercised in the soil mass. Both cases of a tension resistant and a tension non-resistant soil are examined. The problem is dealt with using the kinematic approach of the Yield Design theory (Salençon 1983, 1990). It is shown that the problem can be reduced to a 4-loading parameter one with modified values for $\{N, V, M, f_h\}$, for which best upper bound solutions are sought through the investigation of 3-dimensional geometrical configurations describing virtual failure mechanisms. A bounding surface corresponding to the ultimate combinations of inclined force and moment is plotted in the $\{N, V, M\}$ space for a range of values of the soil inertia body forces, f_h. The results are compared with already available solutions, both for circular footings (e.g. Sekiguchi & Kobayashi, 1997) and strip footings (Salençon & Pecker, 1995a, b), in an attempt to propose a general expression for the description of the obtained bounding surface.

1. INTRODUCTION

In previous works, Cremer, Pecker & Davenne (2001, 2002) introduced the concept of "macro-element" as a numerical tool for a concise and accurate prediction of the response of shallow foundations during time history analyses of structures.

The development of the "macro-element" for the soil-foundation system involves, as a first step, the determination of the yield surface of the system, in the form of a convex surface in the loading parameters space, which makes possible to decide whether or not a bearing capacity failure is reached. The loading parameters of such a problem are usually the resultant vertical force N, the horizontal force V and the moment M acting at the center of the footing, the unit weight of the soil γ and the surcharge q at the soil surface. In the works of Cremer, Pecker & Davenne (2001, 2002), the soil-foundation "macro-element" was developed for the case of a strip footing and the determination of the bearing capacity of the soil-foundation system was reduced to a 2-dimensional plane strain problem. Well established solutions for the form and shape of the yield surface in the $\{N, V, M\}$ space corresponding to the bearing capacity of shallow strip footings and for soils obeying either to the Tresca (*e.g.* Salençon & Pecker 1995a, b) or the Mohr – Coulomb failure criterion (*e.g.* Paolucci & Pecker 1997a, 1997b) were used in establishing the proposed "macro-element". With the goal of enlarging the range of applicability of the "macro-element", the current work aims at extending the results obtained by Salençon & Pecker (1995a, 1995b) for the bearing capacity of strip foundations on cohesive soil, to non plane-strain foundation configurations and specifically to the case of circular footings resting on a homogeneous

purely cohesive isotropic soil with or without resistance to tension.

Concerning the bearing capacity of circular footings, previous results by Salençon (1974) and Salençon & Matar (1982) refer to purely vertical loading with various soil conditions. Segikuchi and Kobayashi (1997) proposed upper and lower bound solutions for the bearing capacity of circular foundations subjected to an eccentric vertical force on clay. Randolph and Puzrin (2003), have reported a complete upper bound yield surface in the $\{N, V, M\}$ space for circular foundations on clay with constant or linearly increasing cohesion. They obtained optimal upper bound solutions by devising non plane-strain failure mechanisms allowing for perfect adhesion in the soil-foundation interface, as is suited for skirted offshore foundations, and they used a recently reported theoretical methodology (Puzrin & Randolph, 2003a, b) for the calculation of the internal rate of plastic work within the mobilized soil volume. Furthermore, Salgado et al. (2004) established upper bound estimates of the maximum vertical force N for circular footings on clays using numerical limit analysis. Finite element solutions of the problem are also reported, as those by Bransby & Randolph (1998), Taiebat & Carter (2000, 2002) or Gouvernec and Randolph (2003), all being oriented towards offshore foundations.

The problem is confronted herein using the kinematic approach of Yield Design theory (Salençon, 1983), thus providing upper bound estimates of the collapse loads of the soil-foundation system.

2. POSITION OF THE PROBLEM

Initial Conception

A rigid circular foundation of radius a is considered, resting on the surface of a homogeneous half-space. The soil-foundation system is subjected to a loading process depending on the loading parameters listed below (see fig. 1), the value of which will determine whether or not a bearing capacity failure will occur in the soil:

a. The resultant vertical force N at the center of the foundation.

b. The resultant horizontal force V at the center of the foundation.

c. The resultant overturning moment M at the center of the foundation.

d. The horizontal seismic soil inertial body force f_h.

e. The vertical seismic soil inertial body force f_v.

f. The soil unit weight γ.

g. The surcharge at the soil surface q.

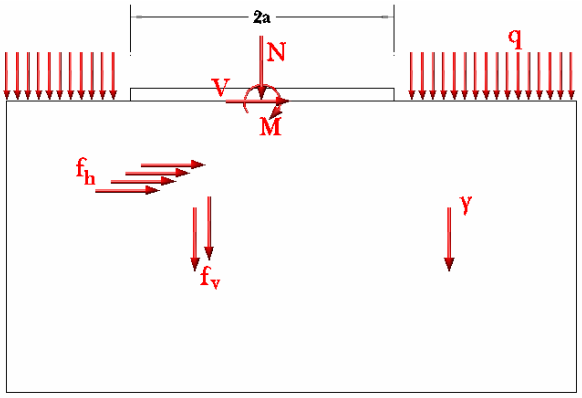

Fig 1: Loading parameters in the problem under consideration

The vertical seismic soil body force f_v can be coupled with the soil unit weight, thus providing an updated vertical unit weight γ^* acting in the soil mass. The loading parameters are thus reduced to six.

Considering that V and M are originated by the inertial response of a superstructure (*e.g.* a single degree of freedom system) to the seismic excitation f_h,

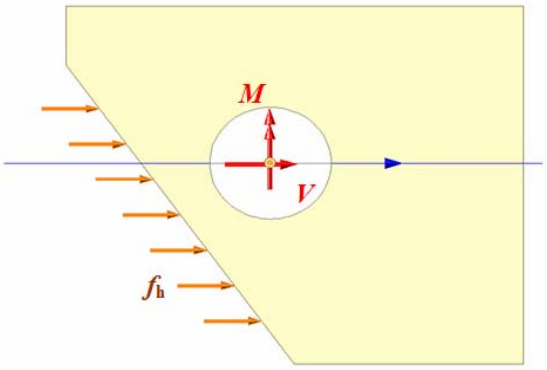

Fig 2: Alignment of horizontal force V, inertial force f_h and moment M in the problem considered

it will be assumed, from now on, that the vector of the horizontal force V and the vector of the horizontal soil inertia forces f_h are collinear, whereas the pseudo-vector of the moment M is perpendicular to this direction as depicted in figure 2.

Failure Criteria

The bearing capacity of the system is dependent among other parameters (*e.g.* geometry, stress path etc.) on the criteria describing the strength of the soil mass and the behavior of the soil-foundation interface. In the following, the failure criteria implemented for the soil and the interface are discussed.

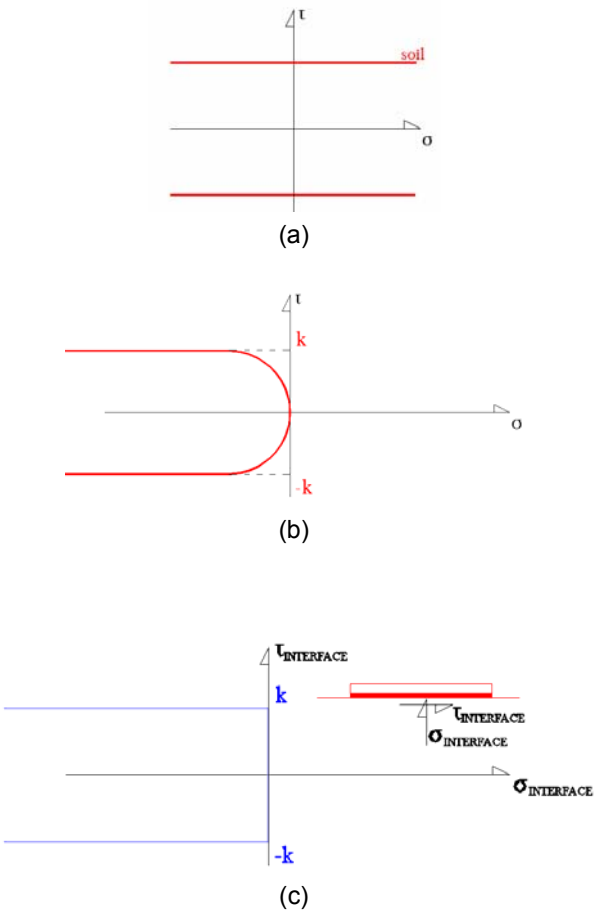

Fig 3: Failure criteria for the soil and the foundation soil-interface: (a) Tresca's criterion; (b) Tresca's criterion with zero tension cut – off; (c) Tresca's criterion for the interface without resistance to tension.

a. *Criteria for the soil.* The isotropic homogeneous soil mass is described as obeying to the Tresca failure criterion with the uniform shear resistance k. Two separate cases are considered:

- Classical Tresca's criterion,
- Tresca's criterion with zero tension cut-off.

These criteria are depicted in figure 3(a, b) in the (σ, τ) space, with σ and τ denoting the normal and tangential stress components acting on any facet within the soil mass.

b. *Criteria for the interface.* The interface is also modeled as obeying the Tresca failure criterion applied to the normal and tangential components (σ, τ) of the stress vector with the same shear resistance k as the resistance of the soil. Moreover, since many foundation failures that were reported after the Mexico City 1985 earthquake (Mendoza & Auvinet, 1988) evidenced uplift and tilt of foundations of buildings or bridges on cohesive soil under earthquake excitations, the interface will not exhibit any resistance to tension for the normal component σ. The criterion for the interface thus obtained is depicted in figure 3c, in the $\{\sigma, \tau\}$ space.

c. *Combination of the soil and interface criteria.* The criteria for the soil and the foundation-soil interface are combined together for the definition of the criterion corresponding to failure on the geometric plane shared by the soil and the interface directly below the foundation (Salençon, 1983). The intersection of the two criteria is shown in figures 4a and 4b.

As is seen in figure 4a, when the soil exhibits resistance to tension, the definition of the criterion for the global interface, *i.e.* the geometric plane below the footing, is governed by the criterion of the interface itself. When a zero tension cut-off is assumed, as in figure 4b, it is the criterion for the soil that governs.

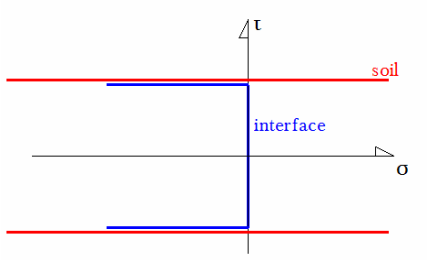

(a)

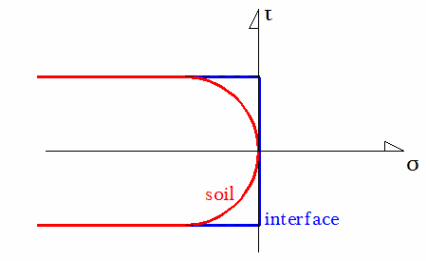

(b)

Fig 4: Combination of soil and interface failure criteria in the plane below the foundation: a) purely cohesive soil; b) purely cohesive soil without resistance to tension.

Taking gravity and surface load into account

a. *Soil unit weight*. Further simplifications arise in the problem by examining the influence of the updated unit weight of the soil on the bearing capacity of the system. In the case of Tresca's criterion, it is classically verified that the updated unit weight of the soil has no influence on the bearing capacity of a circular footing (*e.g.* Salençon, 1983). In the case of a purely cohesive soil with a zero tension cut-off, the effect of the updated unit weight on the bearing capacity of the system is positive as long as the upward vertical accelerations caused by seismic excitations do not exceed the soil own weight. Despite this restriction, since only upper bound estimates for the bearing capacity will be established in the present work, the problem will be studied assuming the updated unit weight of the soil is equal to naught: this conclusion relies on the statement established in (Salençon & Pecker, 1995b) that any upper bound estimate for the bearing capacity on a purely cohesive soil is valid for the soil with the same shear strength and a zero tension cut-off.

b. *Surcharge at the soil surface.* Within the same context, the influence of the surcharge is known to be simply additive for a purely cohesive soil, a result that remains valid for the soil with the same shear strength and a zero tension cut-off, provided that q is downward oriented, what is assumed henceforth.

c. *Conclusions.* The above observations lead to the reduction of the number of loading parameters from six to four, and upper bounds for $(N,\ V,\ M,\ f_h)$ will be established. As soon as such an upper bound $(N^0,\ V^0,\ M^0,\ f_h^0)$ is obtained, the corresponding upper bound for the system with surcharge q and unit weight γ is just $(N^0+qA,\ V^0,\ M^0,\ f_h^0)$.

3. SOLUTION PROCEDURE

Kinematic approach "from outside"

Following Salençon (1983, 1990), the procedure is briefly outlined in a number of steps:

1. In the domain Ω of the examined system (*i.e.* the foundation and the soil half-space), a virtual kinematically admissible velocity field $\underline{\hat{U}}$ is considered. This corresponds to a strain rate tensor $\underline{\underline{\hat{\mathbf{d}}}}$ defined in Ω. It also corresponds to velocity discontinuities $[\![\underline{\hat{U}}]\!]$ defined along jump surfaces Σ in Ω.

2. The resisting rate of work $P_r(\underline{\hat{U}})$ of a stress tensor field $\underline{\underline{\boldsymbol{\sigma}}}$ in this virtual velocity field is given by the equation:

$$(1) \qquad P_r(\underline{\hat{U}}) = \int_\Omega \sigma_{ij}\hat{d}_{ij}\,d\Omega + \int_\Sigma \sigma_{ij}[\![\hat{U}_i]\!]n_j\,d\Sigma$$

where σ_{ij} denote the components of $\underline{\underline{\boldsymbol{\sigma}}}$ and n_j, the components of the unit vector normal to Σ. Summation over repeated indexes is implied. Given the virtual velocity field, the resisting rate of work $P_r(\underline{\hat{U}})$ is maximized over all the stress fields that comply with the strength criteria of the soil and of the interface, through the introduction of the functions π of maximum resisting rate of work. These are derived from the strength criteria as follows.

- *For the soil:*

$$(2)\qquad \begin{cases} \pi\left(\hat{\underline{\underline{\mathbf{d}}}}\right)=\sup\left\{\sigma_{ij}\hat{d}_{ij};f_{\text{soil}}\left(\underline{\underline{\boldsymbol{\sigma}}}\right)\le 0\right\} \\ \pi\left(\underline{n},\left[\!\left[\hat{\underline{U}}\right]\!\right]\right)=\sup\left\{\sigma_{ij}\left[\!\left[\hat{U}_i\right]\!\right]n_j;f_{\text{soil}}\left(\underline{\underline{\boldsymbol{\sigma}}}\right)\le 0\right\} \end{cases}$$

- *For the interface:*

$$(3)\qquad \pi\left(\underline{n},\left[\!\left[\hat{\underline{U}}\right]\!\right]\right)=\sup\left\{\sigma_{ij}\left[\!\left[\hat{U}_i\right]\!\right]\,n_j;f_{\text{interf}}\left(\underline{\underline{\boldsymbol{\sigma}}}\right)\le 0\right\}$$

In (3), f_{interf} denotes the yield function for the interface.

The explicit expression of the functions π for a series of criteria both for continuous media and for interfaces can be found in Salençon, (1983). The following are recalled for the needs of the problem considered here, k denoting the shear strength in the medium:

- *Tresca's criterion*

$$(4a)\qquad \pi\left(\hat{\underline{\underline{\mathbf{d}}}}\right)=\begin{cases}+\infty & \text{if}\quad \operatorname{tr}\hat{\underline{\underline{\mathbf{d}}}}\neq 0\\ k\left(\left|\hat{d}_1\right|+\left|\hat{d}_2\right|+\left|\hat{d}_3\right|\right) & \text{if}\quad \operatorname{tr}\hat{\underline{\underline{\mathbf{d}}}}=0\end{cases}$$

$$(4b)\qquad \pi\left(n,\left[\!\left[\hat{\underline{U}}\right]\!\right]\right)=\begin{cases}+\infty & \text{if}\quad \left[\!\left[\hat{\underline{U}}\right]\!\right]\cdot\underline{n}\neq 0\\ k\left|\left[\!\left[\hat{\underline{U}}\right]\!\right]\right| & \text{if}\quad \left[\!\left[\hat{\underline{U}}\right]\!\right]\cdot\underline{n}=0\end{cases}$$

In the above, $\hat{d}_1$, $\hat{d}_2$ and $\hat{d}_3$ are the principle strain rates of $\hat{\underline{\underline{\mathbf{d}}}}$.

- *Tresca's criterion with zero tension cut-off*

(4c)

$$\pi\left(\hat{\underline{\underline{\mathbf{d}}}}\right)=\begin{cases}+\infty & \text{if}\quad \operatorname{tr}\hat{\underline{\underline{\mathbf{d}}}}<0\\ k\left(\left|\hat{d}_1\right|+\left|\hat{d}_2\right|+\left|\hat{d}_3\right|-\operatorname{tr}\hat{\underline{\underline{\mathbf{d}}}}\right) & \text{if}\quad \operatorname{tr}\hat{\underline{\underline{\mathbf{d}}}}\ge 0\end{cases}$$

(4d)

$$\pi\left(\underline{n},\left[\!\left[\hat{\underline{U}}\right]\!\right]\right)=\begin{cases}+\infty & \text{if}\quad \left[\!\left[\hat{\underline{U}}\right]\!\right]\cdot\underline{n}<0\\ k\left(\left|\left[\!\left[\hat{\underline{U}}\right]\!\right]-\left[\!\left[\hat{\underline{U}}\right]\!\right]\cdot\underline{n}\right)\right| & \text{if}\quad \left[\!\left[\hat{\underline{U}}\right]\!\right]\cdot\underline{n}\ge 0\end{cases}$$

- *Tresca's criterion for the interface without resistance to tension*

(4e)

$$\pi\left(\underline{n},\left[\!\left[\hat{\underline{U}}\right]\!\right]\right)=\begin{cases}+\infty & \text{if}\quad \left[\!\left[\hat{\underline{U}}\right]\!\right]\cdot\underline{n}<0\\ k\left|\left[\!\left[\hat{\underline{U}}\right]\!\right]-\left(\left[\!\left[\hat{\underline{U}}\right]\!\right]\cdot\underline{n}\right)\underline{n}\right| & \text{if}\quad \left[\!\left[\hat{\underline{U}}\right]\!\right]\cdot\underline{n}\ge 0\end{cases}$$

Thus the maximum internal rate of work P_{mr} is given by:

$$(5)\qquad P_{\text{mr}}=\int_{\Omega}\pi\left(\hat{\underline{\underline{\mathbf{d}}}}\right)d\Omega+\int_{\Sigma}\pi\left(\underline{n},\left[\!\left[\hat{\underline{U}}\right]\!\right]\right)d\Sigma$$

3. Given the velocity field $\hat{\underline{U}}$, and for all the loading parameters Q_i (for example we may define $Q_1 = N$, $Q_2 = V$ etc.), the associated kinematic parameters $\dot{q}_i\left(\hat{\underline{U}}\right)$ are determined through The expression of the rate of external work:

$$(6)\qquad P_{\text{ext}}\left(\hat{\underline{U}}\right)=Q_i\dot{q}_i\left(\hat{\underline{U}}\right)$$

4. Provided the fundamental inequality:

$$P_{\text{ext}}\left(\hat{\underline{U}}\right)\le P_{\text{mr}}\left(\hat{\underline{U}}\right)$$

we derive upper bounds to the ultimate limit (or extreme) loads by equating the maximum resisting rate of work $P_{\text{mr}}\left(\hat{\underline{U}}\right)$ to the external rate of work $P_{\text{ext}}\left(\hat{\underline{U}}\right)$ and then calculating the corresponding values for the loading parameters Q_i.

5. Through the examination of a series of kinematically admissible virtual velocity fields, the minimum upper bound is retained as the most satisfactory approach to the exact solution.

Relevant velocity fields

Any kinematically admissible virtual velocity field may be used in the above described

procedure but it comes out obviously that only those kinematically admissible virtual velocity fields for which $P_{\text{mr}}\left(\hat{\underline{U}}\right)$ remains finite shall lead to a valuable upper bound estimate of the extreme loads. This condition implies that both functions π should remain finite at any point of the system. Such virtual velocity fields are named *relevant* (from the Yield Design theory viewpoint) and the corresponding conditions on $\hat{\underline{\underline{\mathbf{d}}}}$ and $\left(\underline{n}, \left[\!\left[\hat{\underline{U}}\right]\!\right]\right)$ are the conditions of relevance, which are derived from the strength criteria only through equations (4). Consequently, the conditions of relevance for a velocity field are formulated as below so that $\pi\left(\hat{\underline{\underline{\mathbf{d}}}}\right) < +\infty$ and $\pi\left(\underline{n}, \left[\!\left[\hat{\underline{U}}\right]\!\right]\right) < +\infty$.

- *Tresca's criterion*

(7a) $\operatorname{tr} \hat{\underline{\underline{\mathbf{d}}}} = 0$

(7b) $\left[\!\left[\hat{\underline{U}}\right]\!\right] \cdot \underline{n} = 0$

- *Tresca's criterion with zero tension cut-off*

(7c) $\operatorname{tr} \hat{\underline{\underline{\mathbf{d}}}} \geq 0$

(7d) $\left[\!\left[\hat{\underline{U}}\right]\!\right] \cdot \underline{n} \geq 0$

- *Tresca's criterion for the interface without resistance to tension*

(7e) $\left[\!\left[\hat{\underline{U}}\right]\!\right] \cdot \underline{n} \geq 0$

Obviously from conditions (7), a relevant virtual velocity field for a Tresca medium with tensile resistance is also relevant for a Tresca medium without tensile resistance, but not vice and versa.

Virtual Mechanisms of failure as sets of virtual velocity fields

It may be proved (under some mathematical assumptions not to be detailed here) that an exhaustive examination of all virtual kinematically admissible (relevant) velocity fields in step 5 of the described solution procedure, would yield the exact solution of the problem and provide the limit loads supported by the system. But such an exhaustive examination is neither possible nor necessary for the practical point of view: only satisfactory upper bounds need being established. To this end, a series of velocity fields is investigated. The virtual fields are grouped in "*mechanisms*" corresponding to a particular pattern of bearing capacity failure of the soil-foundation system. Each virtual mechanism is defined by a number of geometrical parameters, which characterize its shape. The optimization procedure results in finding those values of the geometrical parameters of each mechanism that give rise to the optimal upper bounds and then selecting the minimum among the optimal upper bounds so obtained. In the following section, the mechanisms examined in this study are briefly presented.

4. DESCRIPTION OF THE VIRTUAL FAILURE MECHANISMS

Planar non plane strain mechanisms

Following Puzrin and Randolph (2003a, b) we may characterize the virtual mechanisms under consideration as planar non plane strain ones. The term "planar" refers to the fact that the velocity field is such that an (orthogonal) Cartesian coordinate system $(x,\ y,\ z)$ may be defined, in which the velocity component parallel to an axis is zero: *e.g.* $U_z = 0$. The term "non plane strain" refers to the fact that the non-zero velocities U_x and U_y are functions of z. Figure 5 shows an example of such a mechanism.

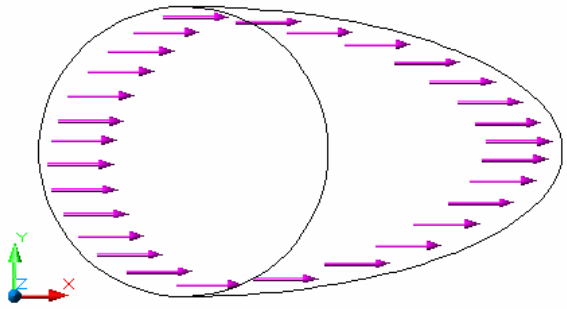

Fig 5: Planar non plane strain mechanism

Translational Mechanism

This virtual mechanism was originally proposed by Green (1954) for combined shear and pressure plane strain problems. It was adapted to a rigid circular footing by Puzrin & Randolph (2003b) by considering that the width of the mechanism in a cross - section normal to the z-axis is proportional to the width of the footing in the same cross - section. This is presented in figure 6. The mechanism is a planar non - plane strain mechanism.

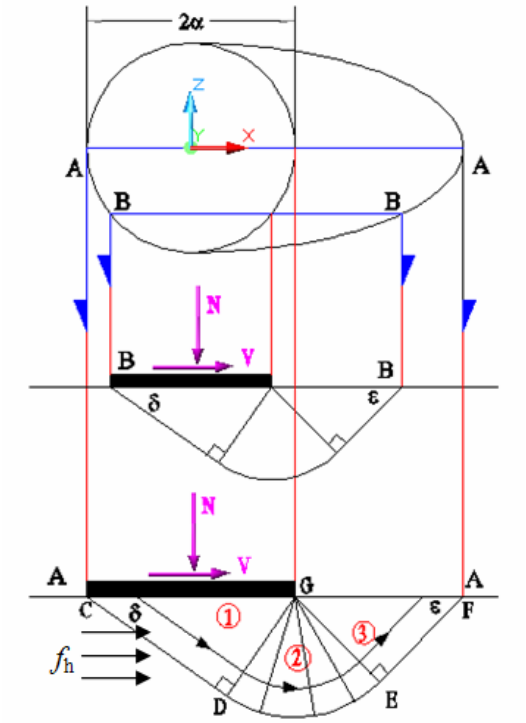

Fig 6: The purely translational mechanism for the bearing capacity of circular footings resting on a Tresca soil.

The mechanism is named "purely translational" as the footing translates rigidly with a virtual velocity $\hat{U}_0$. This velocity is constant in magnitude all along the streamlines of the mechanism. The description of the mechanism involves three zones within the soil mass (fig. 6). In a plane orthogonal to the z-axis, zones (1) and (3) translate rigidly with velocity $\hat{U}_0$ and zone (2) is a circular region in section where pure shear strain rate takes place (shear fan). The resisting rate of work in this virtual mechanism is developed in the volume of zone (2) and on the surface of discontinuity CDEF. The mechanism involves no uplift of the footing. Since there is no rotation of the footing, it does not provide any upper bound in relation with M. The shape of the mechanism is defined by two geometrical parameters: the angles δ and ε, also presented in figure 6 while a 3-dimensional representation of the mechanism is depicted in fig. 7.

With this mechanism Puzrin & Randolph (2003b) computed the equations for the maximum resisting rate of work and gave an upper bound solution in the form of an (N, V) interaction diagram. This solution is extended here with the addition of the effect of the horizontal soil inertia forces f_h.

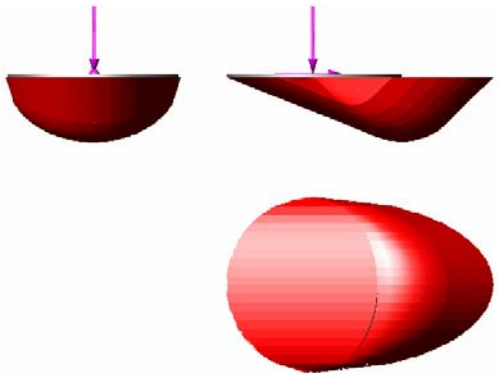

Fig 7: Three – dimensional representation of purely translational mechanism for circular footings on Tresca soils

Purely Rotational mechanism

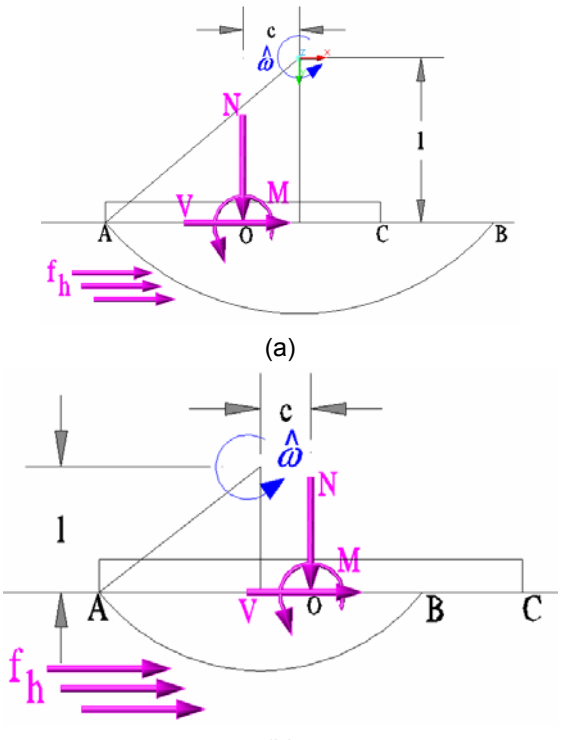

Fig 8: "Purely Rotational mechanism" for circular footings resting on Tresca soils: (a) mechanism without uplift, (b) mechanism with uplift

The plane strain version of this virtual mechanism was studied by Salençon & Pecker (1995a, b). Segikuchi & Kobayashi (1997)

extended this mechanism to a circular footing subjected to an eccentric vertical load N. Herein, the mechanism of Segikuchi & Kobayashi is extended in order to include a horizontal force V and the soil inertial forces f_h.

The rigid circular footing is considered to rotate rigidly around an axis parallel to the z-axis, as depicted in figure 8.

The rotation of the footing induces the rotation of the soil bulk below it as a rigid body, with the same angular velocity $\hat{\omega}$. For this reason, this virtual mechanism is named "purely rotational". Its geometry is described by two geometric parameters: c and l, which define the position of the axis of rotation with respect to the center of the foundation. The mechanism may produce two distinct failure patterns depending on the value of c. These are shown in figure 8(a, b). In pattern (a), there is no uplift of the footing and the resisting rate of work is only produced along the surface of discontinuity AB. In pattern (b), there is uplift of the footing along BC. Thus, a fraction of the total resisting rate of work is produced along the surface of discontinuity AB, and a fraction along the uplift area BC. Figure 9 presents a 3-dimensional representation of the two patterns of the "purely rotational" virtual mechanism.

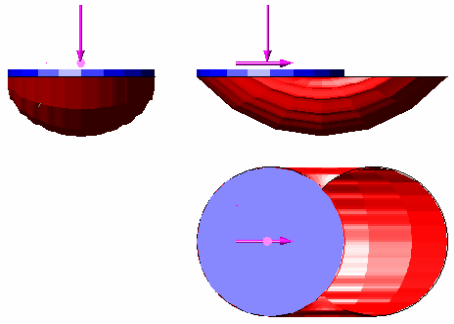

(a)

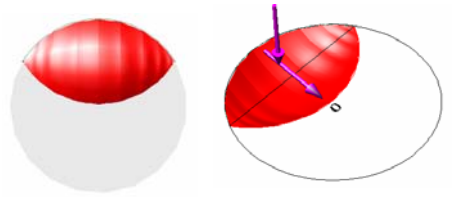

(b)

Fig 9: 3- dimensional representation of the "purely rotational" virtual mechanism for circular footings on Tresca soil: (a) mechanism without uplift; (b) mechanism with uplift.

Rotational Mechanism with shear fan (Shear – rotational)

A third type of virtual mechanism is considered, which will be named "shear – rotational" mechanism. The geometry of this mechanism is depicted in fig. 10. It originates from the work of Salençon & Pecker (1995a, b) on strip foundations. A similar mechanism was also treated by Randolph & Puzrin (2004) for the case of circular foundations with perfect adhesion in the soil-foundation interface.

Failure is induced by rotation of the footing with an angular velocity $\hat{\omega}$ around an axis located within the soil mass and parallel to z-axis. By varying the X coordinate of the axis of rotation with respect to the center of the footing, three different patterns of bearing capacity failure are obtained, which are presented in fig. 10.

Pattern (a) is obtained for $-a \le X \le 0$. Pattern (b) is obtained for $-\infty \le X \le -a$ and pattern (c) for $0 \le X \le a$.

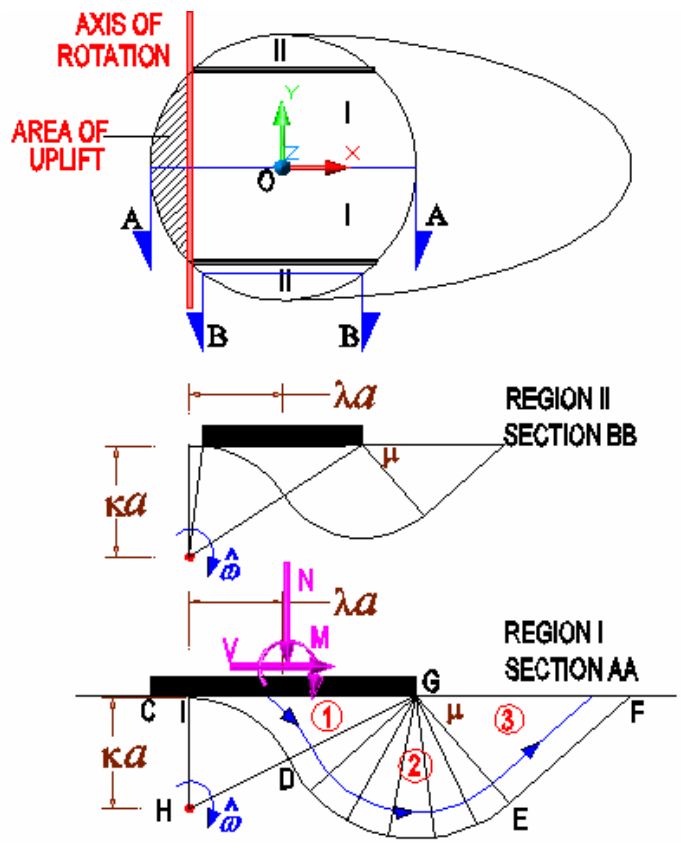

(a)

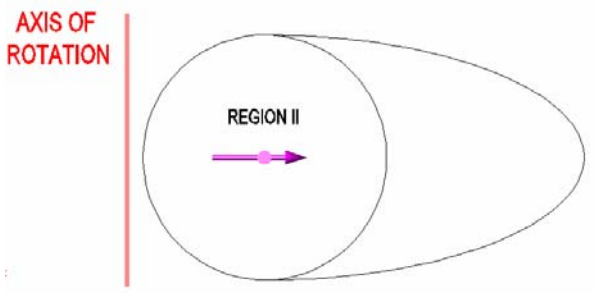

(b)

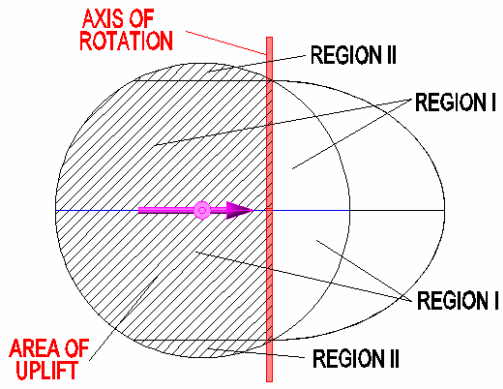

(c)

Fig 10: Failure patterns obtained from the "Shear-rotational" virtual mechanism for circular footings on Tresca's criteria.

For the failure pattern (a), the mobilized soil volume is divided into two distinct regions noted I and II in fig. 10a. In region I, the axis of rotation is found directly below the footing and there is an area where uplift of the footing is observed. In region II, the axis of rotation is found outside the trace of the foundation and there is no uplift.

In both regions I and II of pattern (a), the soil volume mobilized by the foundation rotation is divided in three zones noted (1), (2) and (3) in fig 10a. In zone (1), the soil is attached to the footing and has the same rigid body rotational motion with rate $\hat{\omega}$. Zone (2) is an area of centered circular streamlines in the XY-plane where pure shear is observed (shear fan). In zone (3), the velocity of mobilized soil follows straight streamlines. The magnitude of the velocity, defined by the rotation of the foundation around the axis of rotation, is kept constant along each streamline starting from the footing up to the surface of the soil mass.

The shape of the mechanism is defined by three geometrical parameters: κ, λ and μ. Parameters κ and λ define the position of the axis of rotation: they are normalized with respect to the radius a of the footing; the parameter μ defines the angle in which the streamlines of zone (3) are inclined with respect to the surface of the soil.

For this pattern, the resisting rate of work is produced:

- within the volume of zones (2) and (3) for regions I and II,
- along the discontinuity surface IDEF for regions I and II,
- along the area where uplift of the footing occurs: IC for region I.

For pattern (b), which is presented in fig. 10b, the axis of rotation is located outside the trace of the foundation and the virtual failure mechanism is completely governed by the region II mode of failure; no uplift of the footing is observed. The resisting rate of work is produced:

- within the volumes of zones (2) and (3) (region II),
- along the surface of discontinuity in the soil mass (region II).

For pattern (c) as presented in fig. 10c, which is obtained for strongly eccentric loading, the axis of rotation is located close to the edge of the footing and a large uplift area is observed. The corresponding virtual mechanism consists in: soil failure in region I with uplift of the footing in regions I and II, in the same way as described before. The resisting rate of work is produced:

- within the volumes of zones (2) and (3) in region I,
- along the surface of discontinuity within the soil mass in region I,
- along the area where uplift of the footing occurs in regions I and II.

A three – dimensional representation of the mechanism is presented in figure 11.

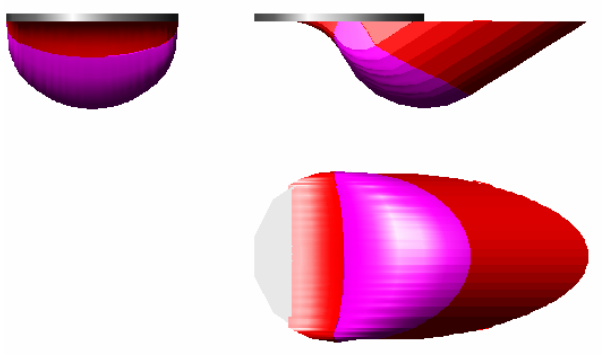

Fig. 11: Three-dimensional representation of the "shear-rotational" virtual mechanism - Pattern (a).

5. SIGNIFICANT POINTS IN THE TREATMENT OF THE VIRTUAL MECHANISMS

Rate of work of external forces

Since the circular footing is assumed to be rigid, any kinematically admissible virtual velocity field $\hat{\underline{U}}$ is due to comply with a rigid body motion of the footing as a boundary condition. For planar velocity fields, such a rigid body motion is defined by the virtual rate of rotation $\hat{\omega}$ and the two components $\hat{U}_{O,X}$ and $\hat{U}_{O,Y}$ of the virtual velocity of the center O of the footing. Consequently the rate of work of external forces acting on the footing in the considered virtual velocity field is just equal to $\left(N\hat{U}_{O,Y}+V\hat{U}_{O,X}+M\hat{\omega}\right)$.

As regards the soil inertia forces, these are assumed to be constant in magnitude and direction all through the soil domain Ω. Thus, the corresponding rate of work is equal to: $f_{\mathrm{h}}\int_{\Omega}\underline{e}_X\cdot\hat{\underline{U}}d\Omega$.

It follows that the complete expression of the rate of work of the external forces

$$P_{\mathrm{ext}}=N\hat{U}_{O,Y}+V\hat{U}_{O,X}+M\hat{\omega}+f_{\mathrm{h}}\int_{\Omega}\underline{e}_X\cdot\hat{\underline{U}}d\Omega$$

may be written in the form of Eq. (6):

$$P_{\mathrm{ext}}=\underline{Q}\cdot\underline{\dot{q}}$$

with the vector of loading parameters:

(8) $$\underline{Q}=\left(N,V,M,f_{\mathrm{h}}\right)$$

and the corresponding vector of associated kinematic parameters

(9) $$\underline{\dot{q}}\left(\hat{\underline{U}}\right)=\left(\hat{U}_{O,Y},\hat{U}_{O,X},\hat{\omega},\int_{\Omega}\underline{e}_X\cdot\hat{\underline{U}}d\Omega\right)$$

Maximum resisting rate of work

Given the virtual velocity field in the soil-foundation domain, the maximum resisting rate of work comes from three contributions, namely:

- within the soil volume, in the zones where soil shearing occurs,
- along the velocity discontinuity surfaces,
- in the areas where uplift of the footing is observed.

a. *Soil Volume*. For the determination of the maximum resisting rate of work via the functions $\pi\left(\hat{\underline{\underline{\mathbf{d}}}}\right)$ as given in Salençon (1983), the evaluation of the principle values $\hat{d}_1$, $\hat{d}_2$ and $\hat{d}_3$ of the strain rate tensor $\hat{\underline{\underline{\mathbf{d}}}}$ corresponding to the assumed velocity field, is necessary. This is achieved using the methodology presented recently by Puzrin & Randolph (2003a, b), which is based upon the use of curvilinear coordinates, one family of which follows the streamlines of the considered virtual velocity field. To this end, the volume of mobilized soil is divided into separate zones according to the geometry of the concerned velocity streamlines. For example, the "translational" mechanism is split into three zones, whereas the "purely rotational mechanism" comprises just one zone. The streamlines (and consequently the soil volume zones) encountered in this study are of two kinds only:

i. Straight streamlines.
ii. Circular streamlines.

These are depicted in figure 12. For each of these two cases a coordinate transformation is considered from the global coordinate orthogonal Cartesian system (X, Y, z) to a local system (x, y, z), which in the present case turns out to be orthogonal, in such a way that, for each zone, the velocity in the mechanism is always parallel to the new local axis x. This results in a translation-rotation of the global system, in the case of straight streamlines and in a transformation to a system of cylindrical coordinates, in the case of circular streamlines.

The global and local coordinate systems for each case are also presented in figure 12.

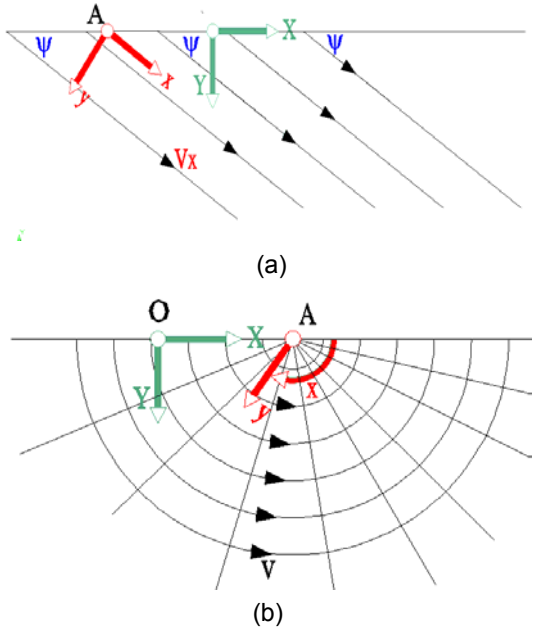

Fig 12: Types of streamlines treated: (a) Straight streamlines and (b) circular streamlines and relevant coordinate transformations.

In the new local coordinate systems we have $U_z = U_y = 0$, and only U_x is a function of y and z. Puzrin and Randolph (2003a, b) explain how this simplifies the determination of the components of the strain rate tensor $\hat{\underline{\underline{\mathbf{d}}}}$ and give analytical expressions for their evaluation for a number of cases, the straight and circular streamlines cases included. It is noted that for all mechanisms considered $\mathrm{tr}\,\hat{\underline{\underline{\mathbf{d}}}} = 0$, and therefore no differentiation is to be made between the two cases of Tresca's criteria for the calculation of maximum resisting rate of work within the soil volume.

b. *Surface of discontinuity*. On the surface of discontinuity between the mobilized and motionless soil there is also a contribution to the maximum resisting rate of work. In all mechanisms considered, the velocity remains tangent to the surface of discontinuity, thus satisfying conditions (7) and providing the same value of maximum resisting rate of work for both cases of Tresca's criteria, which is computed as the integral of the relevant function $\pi\left(\underline{n}, [\![\underline{\hat{U}}]\!]\right)$ on the velocity discontinuity surface.

c. *Area with uplift of the footing*. Whenever uplift of the foundation is predicted according to the virtual mechanism of failure, a fraction of the total maximum resisting rate of work is produced in the corresponding area. Emphasis should be put on the differentiation of the maximum resisting rate of work developing on the uplift area of the foundation according to whether the soil is tension resistant or not. As explained in section 2, when the soil is tension resistant, the global yield function for the interface, exactly below the foundation is obtained from the yield function of the interface and the relevant function $\pi\left(\underline{n}, [\![\underline{\hat{U}}]\!]\right)$ for the calculation of internal rate of plastic work in the detachment area is equation (4e) (cf. Fig. 13a) :

$$\pi\left(\underline{n}, [\![\underline{\hat{U}}]\!]\right) = \begin{cases} +\infty & \text{if} \quad [\![\underline{\hat{U}}]\!] \cdot \underline{n} < 0 \\ k\left|[\![\underline{\hat{U}}]\!] - \left([\![\underline{\hat{U}}]\!] \cdot \underline{n}\right)\underline{n}\right| & \text{if} \quad [\![\underline{\hat{U}}]\!] \cdot \underline{n} \geq 0 \end{cases}$$

On the contrary, if the soil obeys the Tresca criterion with a zero tension cut-off, the global yield function is given by Eq. (4d) (cf. Fig. 13b):

$$\pi\left(\underline{n}, [\![\underline{\hat{U}}]\!]\right) = \begin{cases} +\infty & \text{if} \quad [\![\underline{\hat{U}}]\!] \cdot \underline{n} < 0 \\ k\left([\![\underline{\hat{U}}]\!] - [\![\underline{\hat{U}}]\!] \cdot \underline{n}\right) & \text{if} \quad [\![\underline{\hat{U}}]\!] \cdot \underline{n} \geq 0 \end{cases}$$

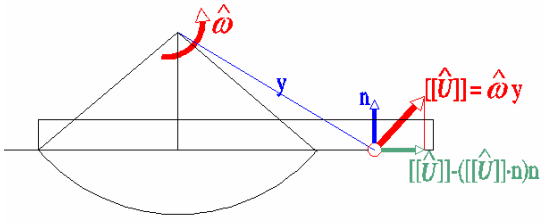

(a)

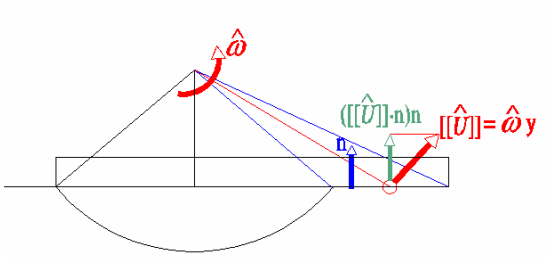

(b)

Fig 13: Calculation of the maximum resisting rate of work on the areas with uplift of the footing: (a) Tension resistant soil and (b) Tension non-resistant soil.

6. RESULTS

Normalization of limit loads

Considering the case of a circular footing of diameter a, resting on a soil exhibiting a shear strength k, the limit loads of the soil – foundation system are normalized with respect to the following scheme:

(10a) $\mathbf{n} = \dfrac{N}{k\pi a^2}$: [Normalized vertical load]

(10b) $\mathbf{v} = \dfrac{V}{k\pi a^2}$: [Normalized horizontal force]

(10c) $\mathbf{m} = \dfrac{M}{2k\pi a^3}$: [Normalized moment]

(10d) $\mathbf{f_h} = \dfrac{\gamma S_a}{k\pi a^2}$: [Normalized inertial forces]

The quantities **n, v, m** defined in (10a, b, c) are dimensionless. On the contrary $\mathbf{f_h}$ has units [m^{-3}], since it represents the magnitude of inertial forces per unit volume and is further integrated over the volume.

It is important to investigate the possible maximum and minimum values that the inertial forces $\mathbf{f_h}$ may take in a real application. These values are useful to define a range of potential values for $\mathbf{f_h}$ used in the presentation of the results. The following table presents the extreme values considered for the quantities involved in the definition of $\mathbf{f_h}$ and subsequently the maximum value obtained for $\mathbf{f_h}$ for real applications.

Table 1: Minimal and maximal values for normalized inertial forces $\mathbf{f_h}$ in practical applications.

Quantity	Symbol	Units	Minimum Value	Maximum Value
Soil Unit Weight	γ	**[KN/m^3]**	15.0	25.0
Horizontal Peak Ground Acceleration	S_a	**[g]**	0.0	1.5
Foundation Radius	a	**[m]**	1.0	10.0
Area of footing	A	**[m^2]**	3.1	314.1
Soil Cohesion	k	**[KPa]**	20.0	200.0
Range of $\mathbf{f_h}$	$\mathbf{f_h}$	**[m^{-3}]**	**0.00**	**0.60**

It should be emphasized that, in principle, soil - foundation failure may be induced just by the action of soil inertial forces, even for very low vertical, horizontal or moment loads. However, the maximal value of $\mathbf{f_h}$ for practical applications has been found smaller than the one inducing soil failure for the analyzed mechanisms.

Organization of results

The results are organized in three sections. The first section deals with the case of a tension resistant soil, the second section with the case of a tension non-resistant soil and the third section briefly compares the results for the two aforementioned cases. For the first two sections, a number of plots and diagrams is presented. These include the following:

- A representation of the failure surface of the soil – foundation system in the **{n, v, m}** space for two different values of $\mathbf{f_h}$, namely $\mathbf{f_h}$ = 0 and 0.5 [m^{-3}]. The first value corresponds to aseismic loading of the footing whereas the second corresponds to severe earthquake foundation loading.
- The interaction diagram **n** – **v** for zero moment loading (**m** = 0) and for three representative values of $\mathbf{f_h}$. These are $\mathbf{f_h}$ = 0, 0.25 and 0.5 [m^{-3}] and they correspond to aseismic loading, moderate earthquake loading and severe earthquake loading respectively.
- The interaction diagram **n** – **m,** with zero horizontal force loading (**v** = 0) and for $\mathbf{f_h}$ = 0, 0.25, 0.5 [m^{-3}].
- The interaction diagram **m** – **v**, for two representative values of the normalized vertical force **n** and for $\mathbf{f_h}$ = 0, 0.25, 0.5 [m^{-3}]. The representative values of the normalized vertical force **n,** for which the interaction diagram **m – v** is presented, are chosen as follows: given the exact maximum vertical centered force for $\mathbf{f_h}$ = 0 on a circular footing resting on a Tresca half - space, being equal to

(11) $$N_{\max}{}^0 = 6.07k\pi a^2 \Rightarrow \mathbf{n}_{\max}{}^0 = 6.07,$$

the selected values of **n** for the **m – v** diagram**,** correspond to global safety factors against bearing capacity failure, equal to FS = 1.5 and FS = 3. These values for FS lead to two values for **n**, namely **n** ≈ 4 and **n** ≈ 2 respectively and correspond to a foundation design with very low conservatism (FS = 1.5) and a conventional foundation design (FS = 3).

Each of the interaction diagrams is constructed as follows: initially, points representing the calculated upper bounds

associated to each mechanism are plotted on the diagram for the values of $\mathbf{f_h}$ selected. These are presented by a distinct marker for each mechanism and by a distinct color for each value of $\mathbf{f_h}$.

Then, the curve joining the optimal upper bounds is plotted for the three values of $\mathbf{f_h}$, obtaining an approximate cross – section of the failure surface in **{n, v, m}** space. Thus, the plotted curves contain information both on the values of the limit loads and on the mechanisms by which these values are obtained.

It is noted that in the legends of the diagrams presented below the translational mechanism is noted as "TR", the purely rotational mechanism as "P/R" and the shear rotational mechanism as "S/R".

Comparison with adapted Eurocode 8 equation. The diagrams for the tension non-resistant material also include a curve which corresponds to the EC8 equation for the seismic bearing capacity of strip foundations on cohesive soils. The EC8 equation is the following:

(12)

$$\frac{\left(1-e\overline{F}\right)^{c_T}\left(\beta\overline{V}\right)^{c_T}}{\left(\overline{N}\right)^{a}\left[\left(1-m\overline{F}^{k}\right)^{k'}-\overline{N}\right]^{b}}+\frac{\left(1-f\overline{F}\right)^{c'_M}\left(\gamma\overline{M}\right)^{c_M}}{\left(\overline{N}\right)^{c}\left[\left(1-m\overline{F}^{k}\right)^{k'}-\overline{N}\right]^{d}}-1\le 0$$

The quantities $\overline{N},\overline{V},\overline{M}$ are the normalized loading parameters defined in the previous context, which have been further normalized with respect to the maximum vertical centered force of a strip footing, $N_{\max}{}^{0}=5.14kB$; B is the width of the footing; $\overline{F}$ is the normalized inertial force in the soil given by $\overline{F}=\rho\mathbf{a}/Bk$, ρ being the mass density of the soil and $\mathbf{a}$ the earthquake-induced soil acceleration. The other quantities appearing in (12) are numerical parameters, the values of which are given below:

Table 2: Values of fixed parameters of equation (12).

a	0.70	***e***	0.21	***k'***	1.00	***β***	2.57
b	1.29	***f***	0.44	c_T	2.00	***γ***	1.85
c	2.14	***m***	0.21	c_M	2.00		
d	1.81	***k***	1.22	c_M'	1.00		

The above solution of EC8 for strip footings is modified for circular footings by changing the value of $N_{max}{}^{0}$ from $5.14kB$ to $6.07k\pi a^2$, which is the exact solution for circular footings. The remaining parameters are kept unchanged, in an attempt to verify the hypothesis, that the shape of the failure surface in the **{n, v, m}** space is the same for strip and circular footings (Bransby & Randolph, 1998).

Finally, in the third section, the **n – v** and **n – m** diagrams for tension resistant and tension non-resistant materials are plotted together in order to emphasize on the differences between the two examined cases.

Section A - Tension resistant Tresca material

Circular footing on tension resistant Tresca material.
Yield surface in the {**n, v, m**} space for $\mathbf{f_h} = 0\mathrm{m}^{-3}$.

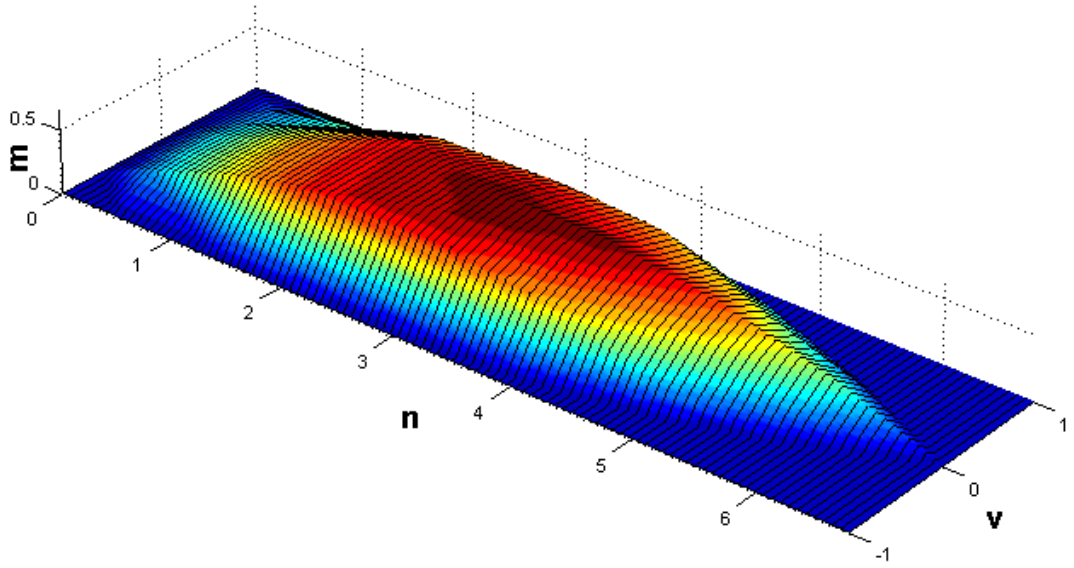

Circular footing on tension resistant Tresca material.
Yield surface in the {**n, v, m**} space for $\mathbf{f_h} = 0.5\mathrm{m}^{-3}$.

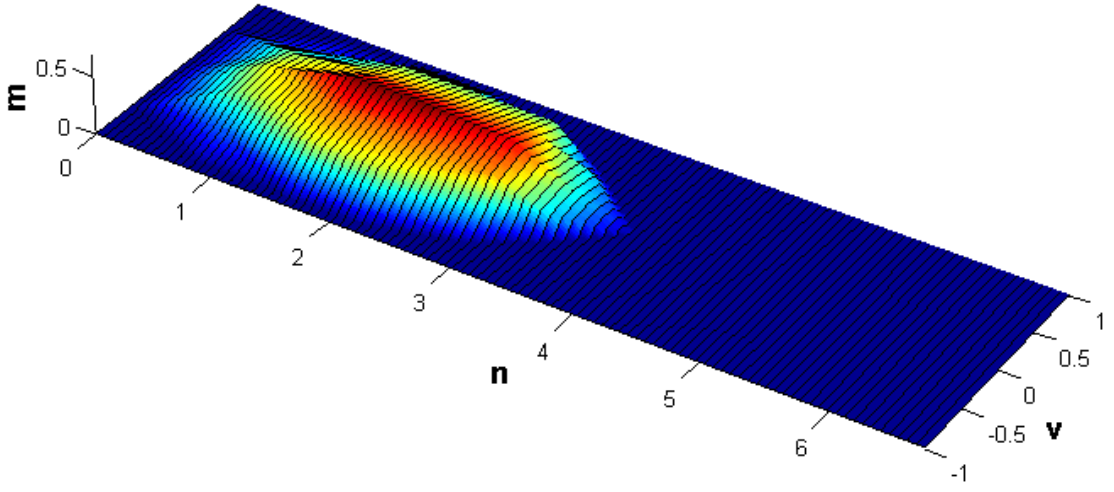

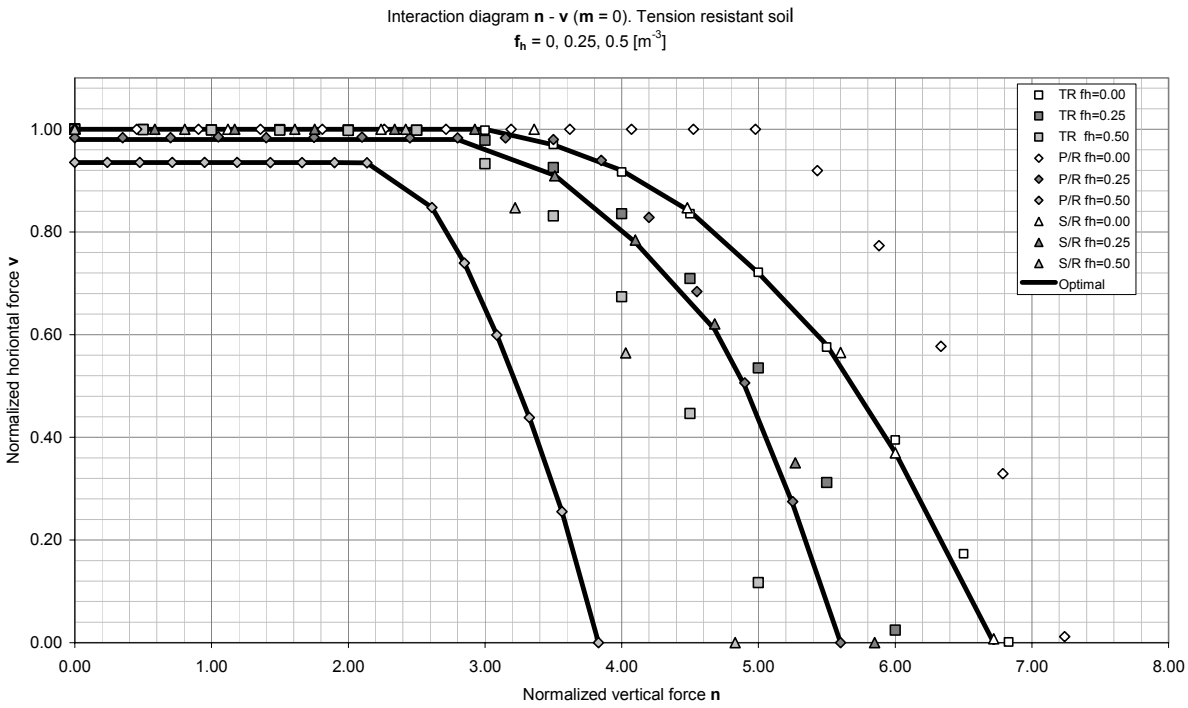
Interaction diagram n - v (m = 0). Tension resistant soil
f_h = 0, 0.25, 0.5 [m^-3]
TR fh=0.00
TR fh=0.25
TR fh=0.50
P/R fh=0.00
P/R fh=0.25
P/R fh=0.50
S/R fh=0.00
S/R fh=0.25
S/R fh=0.50
Optimal
Normalized horiontal force v
Normalized vertical force n
0.00
0.20
0.40
0.60
0.80
1.00
0.00
1.00
2.00
3.00
4.00
5.00
6.00
7.00
8.00

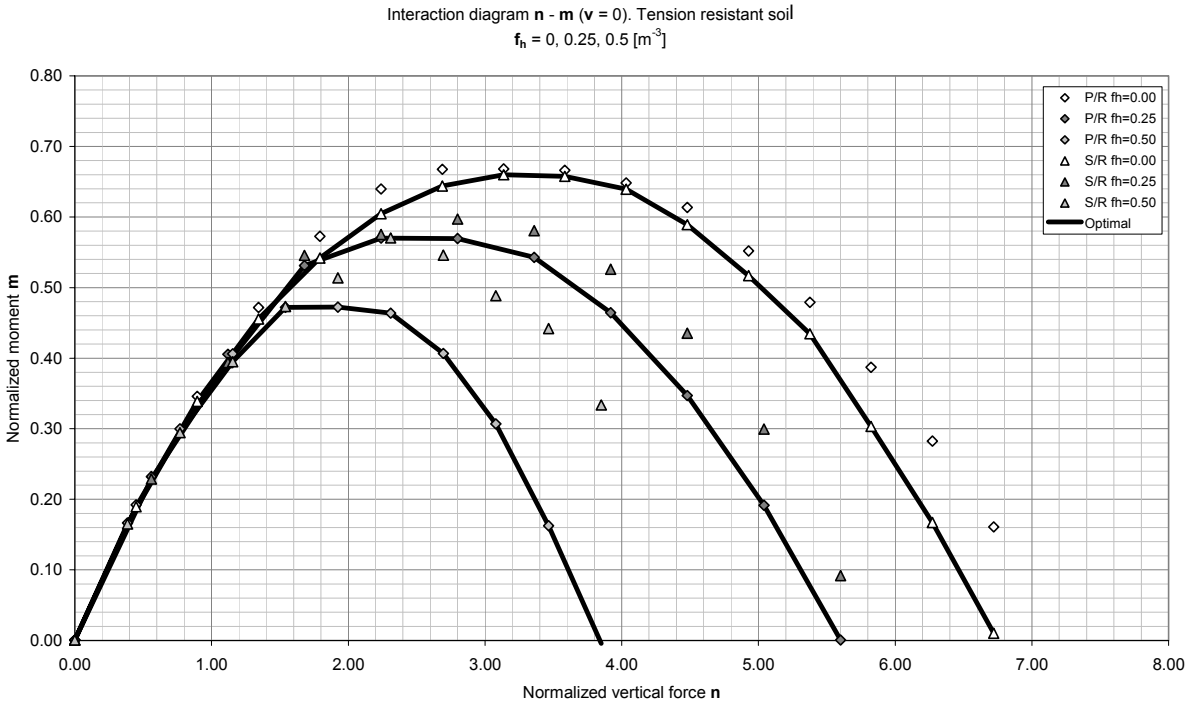
Interaction diagram n - m (v = 0). Tension resistant soil
f_h = 0, 0.25, 0.5 [m^-3]
P/R fh=0.00
P/R fh=0.25
P/R fh=0.50
S/R fh=0.00
S/R fh=0.25
S/R fh=0.50
Optimal
Normalized moment m
Normalized vertical force n
0.00
0.10
0.20
0.30
0.40
0.50
0.60
0.70
0.80
0.00
1.00
2.00
3.00
4.00
5.00
6.00
7.00
8.00

Interaction diagram **m** - **v** (**n** = $\mathbf{n_{max}^0}$/3). Tension resistant soil

$\mathbf{f_h}$ = 0, 0.25, 0.5 [m^{-3}]

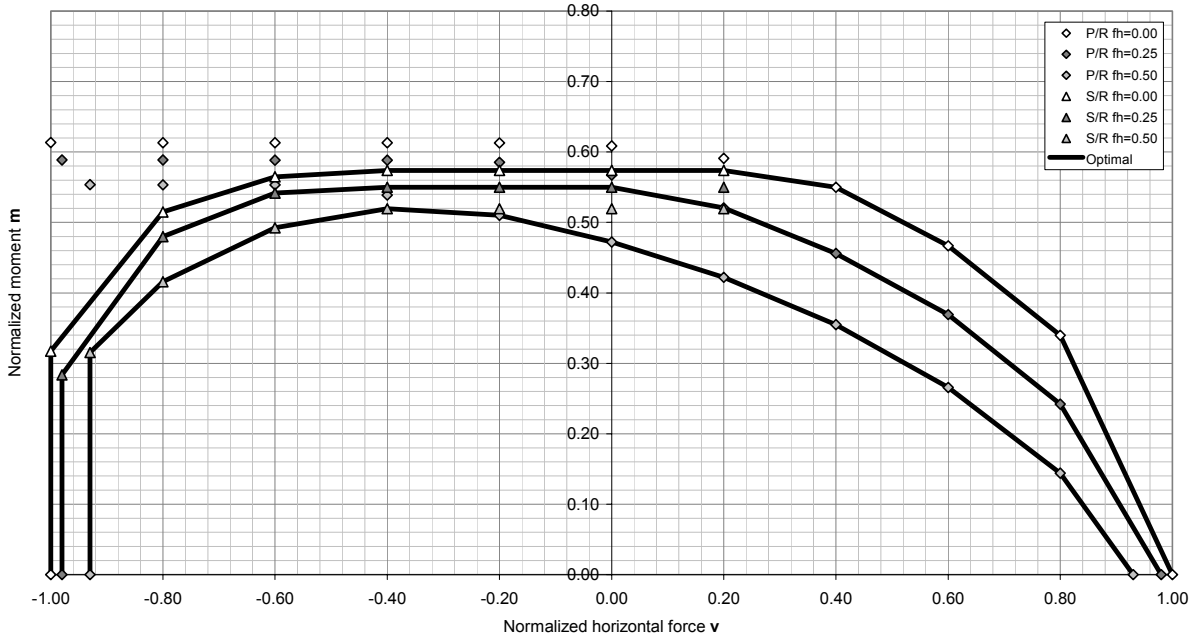

Interaction diagram **m** - **v** (**n** = $\mathbf{n_{max}^0}$/1.5). Tension resistant soil

$\mathbf{f_h}$ = 0, 0.25 [m^{-3}]

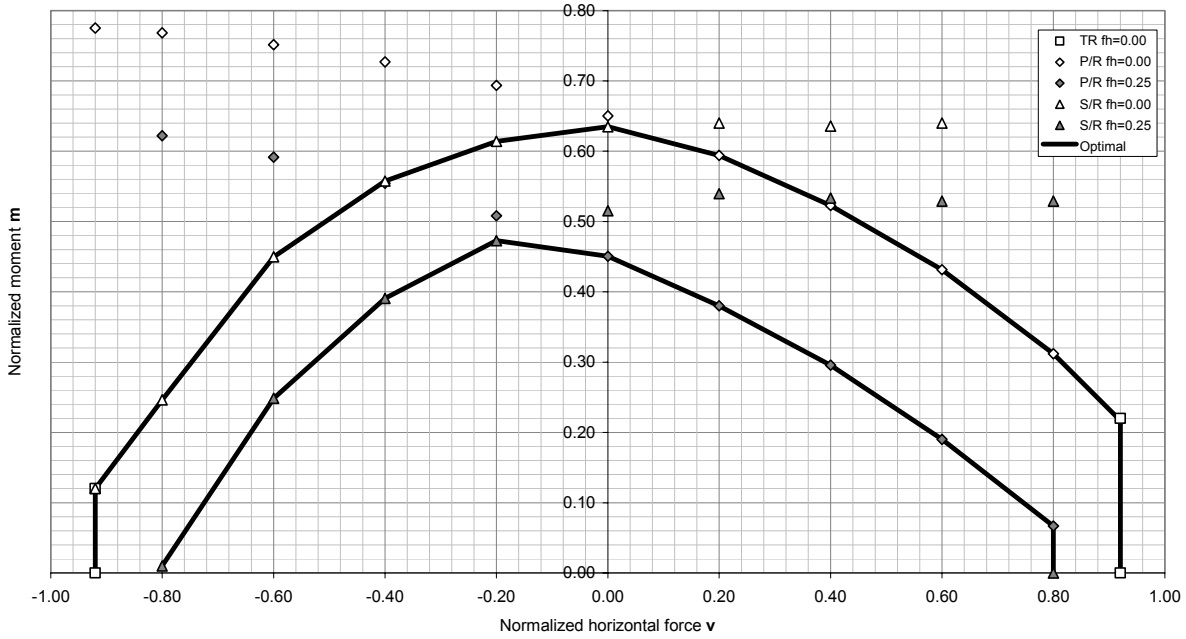

Section B - Tension non-resistant Tresca material

Circular footing on tension non-resistant Tresca material.
Yield surface in the {**n, v, m**} space for $\mathbf{f_h} = 0m^{-3}$.

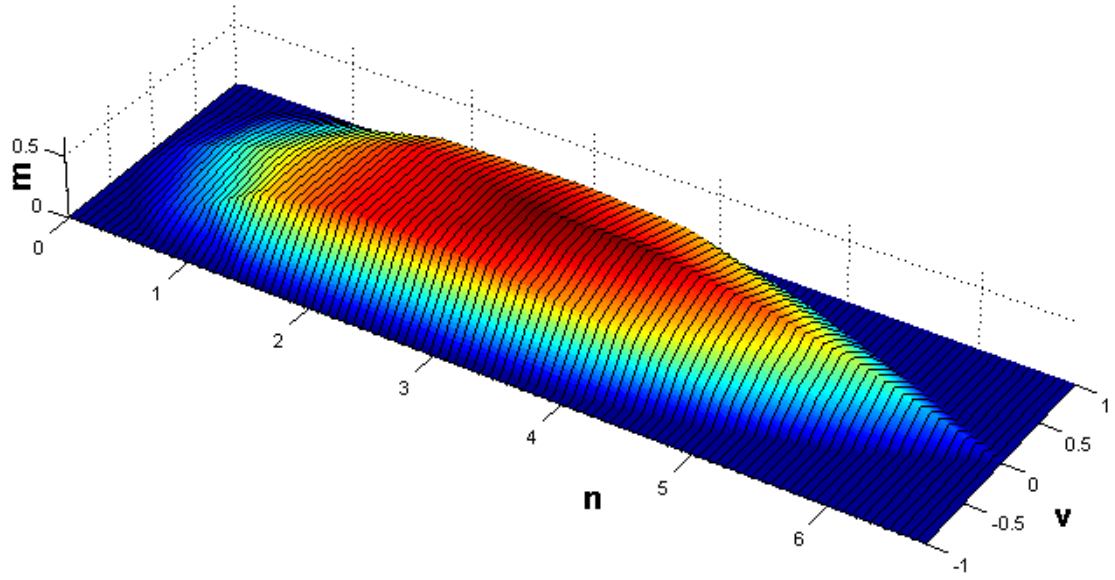

Circular footing on tension non-resistant Tresca material.
Yield surface in the {**n, v, m**} space for $\mathbf{f_h} = 0.5m^{-3}$.

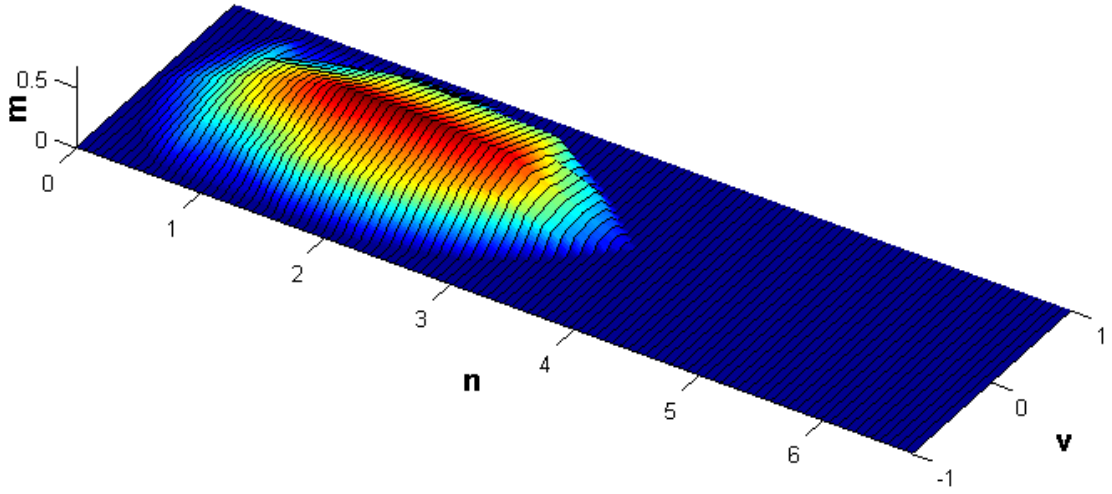

Interaction diagram **n** - **v** (**m** = 0). Tension non-resistant soil
$\mathbf{f_h}$ = 0, 0.25, 0.5 [m^{-3}]

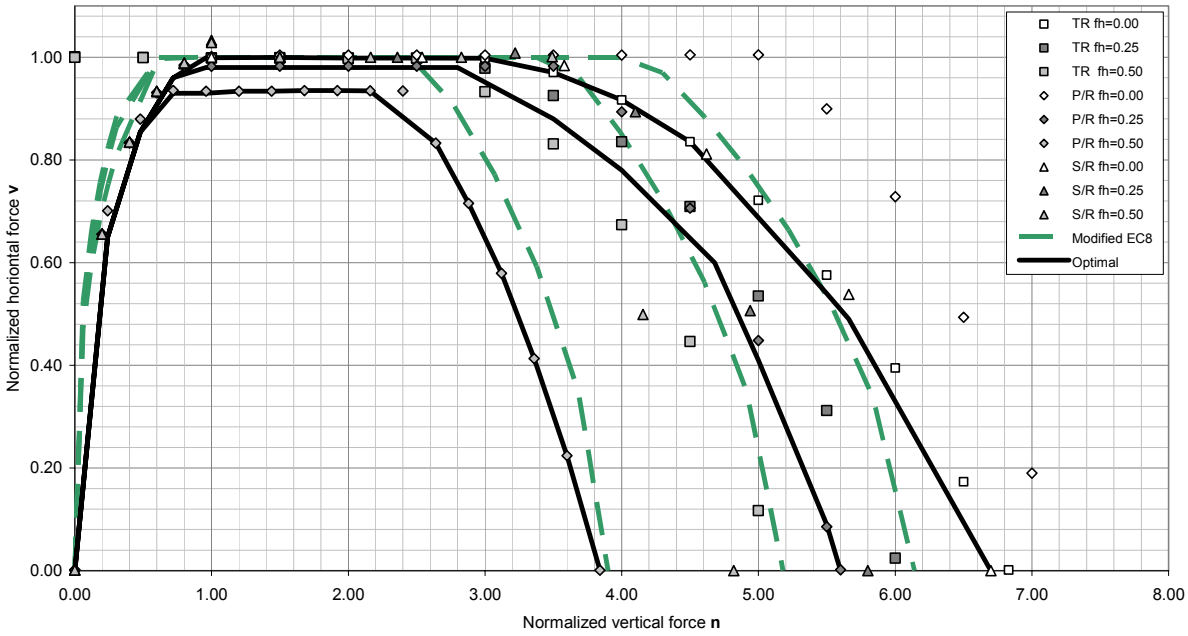

Interaction diagram **n** - **m** (**v** = 0). Tension non-resistant soil
$\mathbf{f_h}$ = 0, 0.25, 0.5 [m^{-3}]

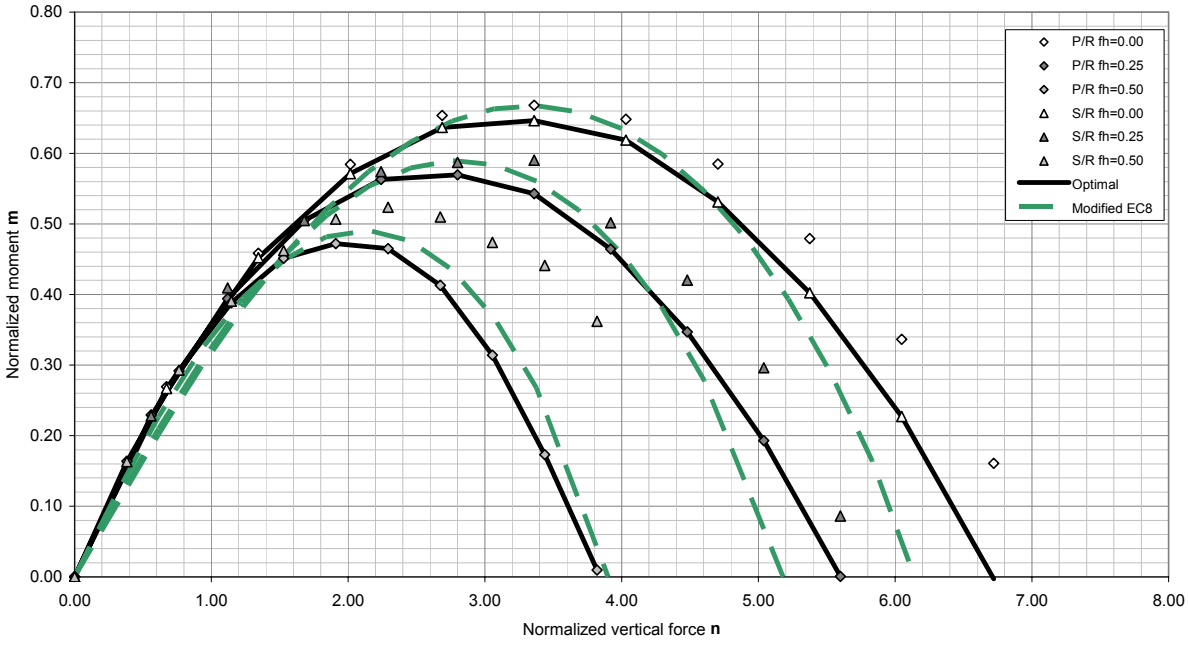

Interaction diagram **m** - **v** (**n** = $\mathbf{n_{max}}^{0}$/3). Tension non-resistant soil

$\mathbf{f_h}$ = 0, 0.25, 0.5 [m^{-3}]

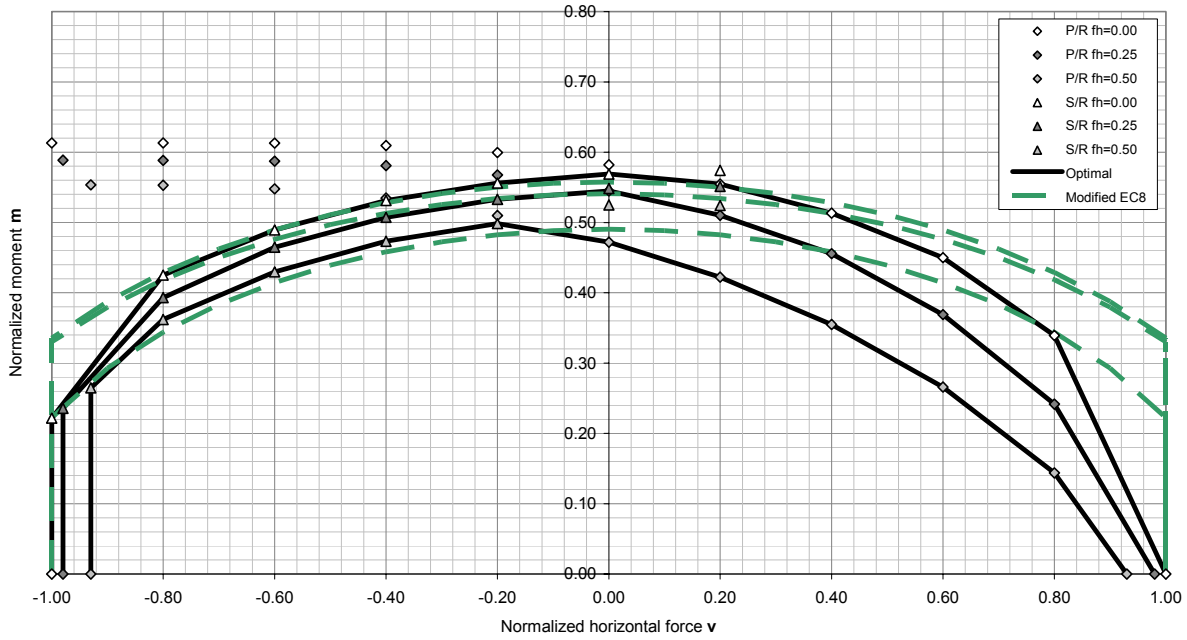

Interaction diagram **m** - **v** (**n** = n_{max}^{0}/1.5). Tension non-resistant soil

$\mathbf{f_h}$ = 0, 0.25 [m^{-3}]

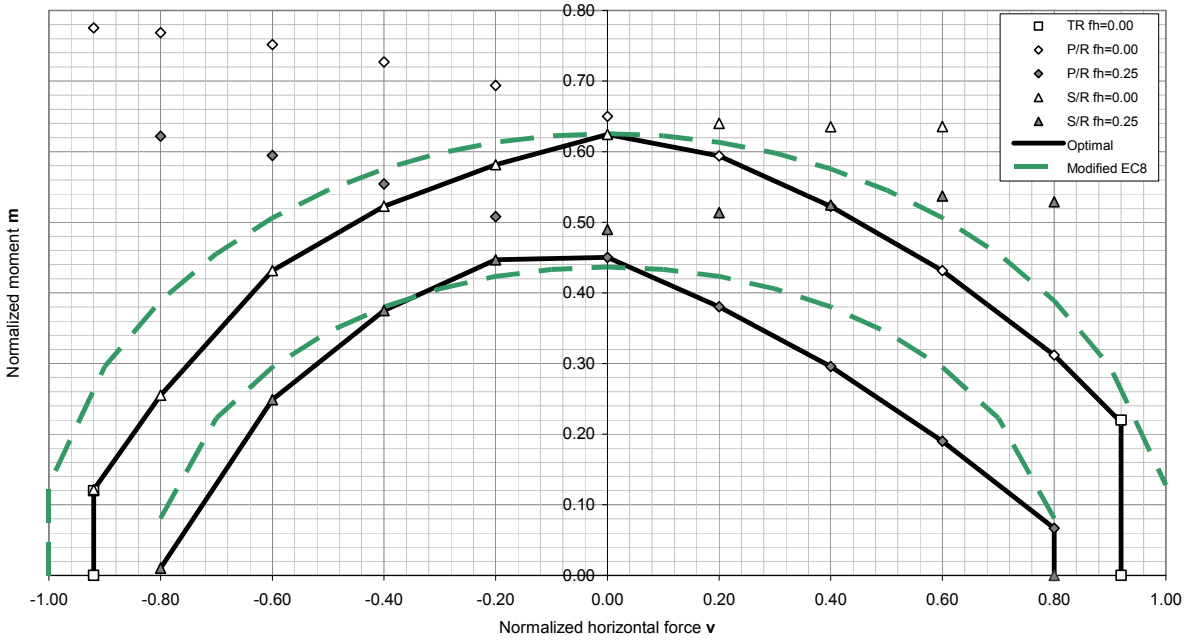

Comparison of tension resistant and tension non-resistant Tresca material

Comparison of results for tension resistant and tension non-resistant Tresca material.
Interaction diagram **n - v**, **m**=0, $\mathbf{f_h}$=0, 0.25, 0.5 [m^{-3}]

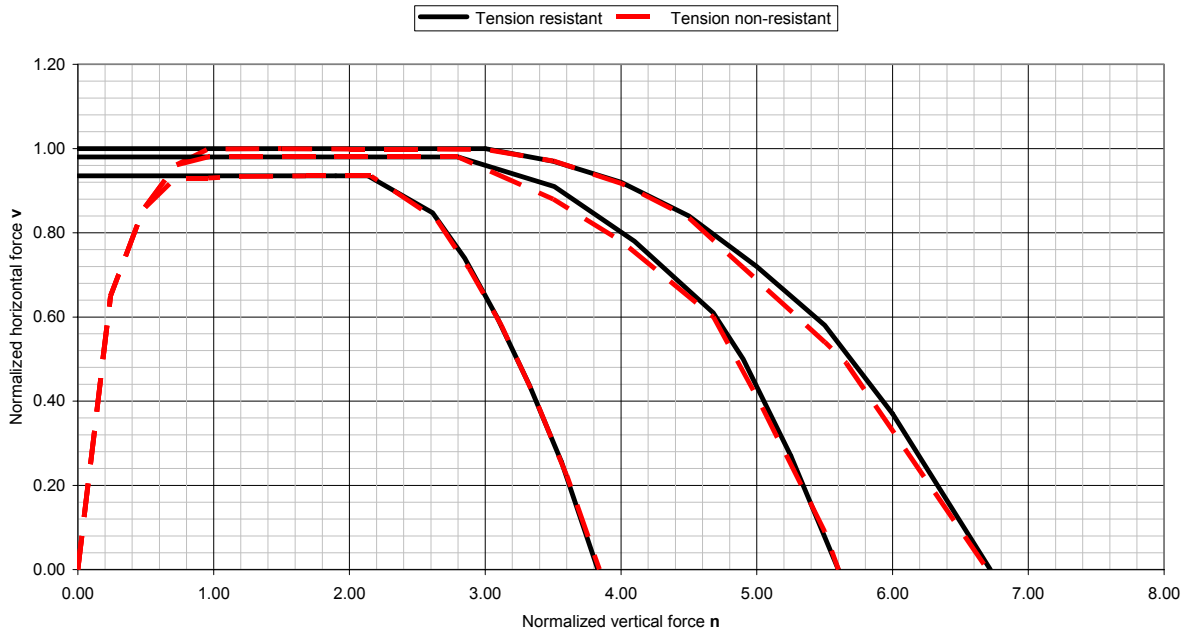

Comparison of results for tension resistant and tension non-resistant Tresca material.
Interaction diagram **m - n, v** = 0, $\mathbf{f_h}$ = 0, 0.25, 0.5 [m^{-3}]

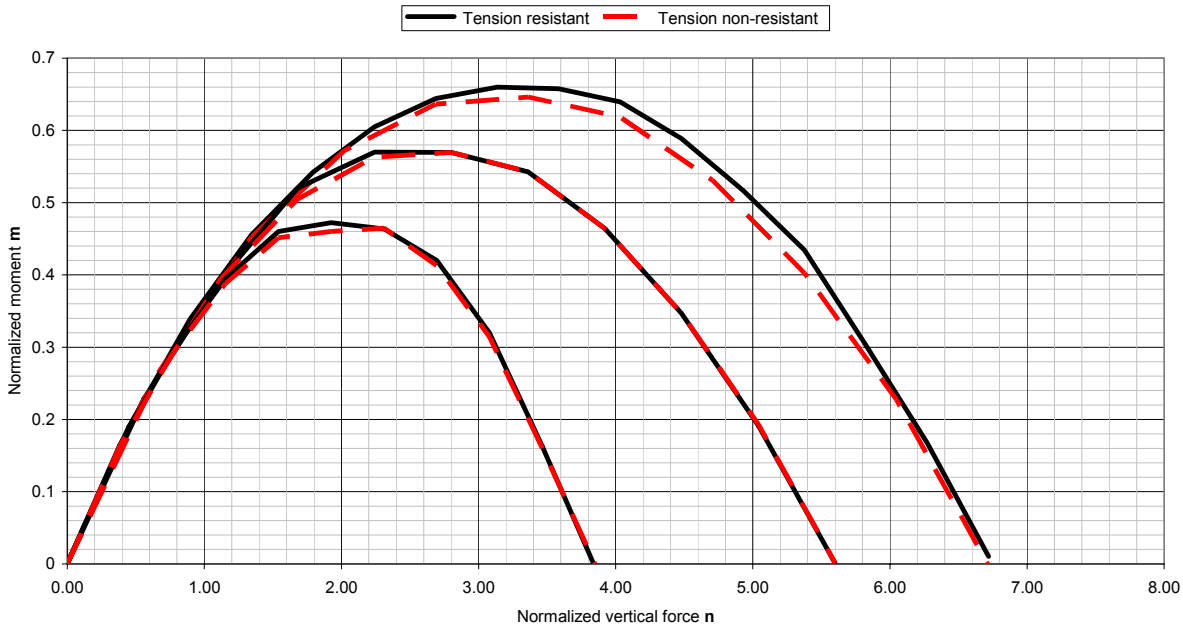

Comments on the results

Examination of the above diagrams leads to the following comments and conclusions:

- The failure surface representation in **{n, v, m}** space or the **n – v** and **n – m** interaction diagrams show that the soil inertia effects are negligible for small values of **n** (corresponding to FS > 2.5), but very significant for high values of **n** (corresponding to FS < 2.0). This is in agreement with previous results (*e.g.* Paolucci & Pecker, 1997a) and with case histories from previous earthquake events, as for instance the 1985 Mexico City earthquake, where foundations designed with low factors of safety suffered bearing capacity failure (Mendoza & Auvinet, 1988). Accordingly, effects of soil inertia forces are significant on the maximum value of the normalized vertical force (45% decrease for $\mathbf{f_h}$ = 0.5) whereas they are negligible on the maximum value of normalized horizontal force or normalized moment (only 6% decrease for $\mathbf{f_h}$ = 0.5), which occur for smaller values of the vertical normalized force (*i.e.* larger safety factors).

- The adequacy of the proposed solution to represent the exact ultimate loads needs to be validated by other means, like a lower bound approach or experimental results, which are scarce for seismic loading. The $N_{max}^{\ 0}$ obtained herein is equal to $N_{max}^{\ 0}$ = 6.72, which is 10% larger than the exact value $N_{max}^{\ 0}$ = 6.07. However, based on the comparison of upper and lower bound solutions for the restriction of the present mechanisms to plane strain conditions (Salençon & Pecker, 1995a, b), the accuracy of the results for combined loading is expected to be acceptable from an engineering standpoint; this results from the construction of the mechanisms which involve a work of the external forces: horizontal force, moment on the footing and acceleration in the soil volume. It can thus be estimated that the computed upper bounds should not overestimate the ultimate load by more than 10%.

- All the mechanisms contribute to the definition of the optimal curves. The translational mechanism is the leading one (together with the shear rotational mechanism) for zero moment loading and small levels of inertial forces. For horizontal force and moment of the same sign, the leading mechanism is the purely rotational mechanism, whereas for horizontal force and moment of different sign, it is the shear rotational mechanism. Also, the larger the value of $\mathbf{f_h}$, the more the failure surface is governed by the purely rotational mechanism.

- In terms of symmetry of the failure surface with respect to the **m** axis**,** the larger the value of **n,** the more symmetric the diagram **m – v**. Also, the smaller the value of $\mathbf{f_h}$, the more symmetric the diagram **m – v**. These observations, derived from an examination of the presented **m – v** diagrams are consistent with those made for strip foundations (Salençon & Pecker, 1995a, b).

- For the tension non-resistant material, the modified EC8 solution is very close to the solution established herein. This supports the observation - hypothesis that the shapes of the failure surfaces for strip and circular footings in the {**n, v, m**} space is very similar (Bransby & Randolph, 1998). It also allows for a potential application of the equation suggested in EC8 for circular footings on cohesive materials by just correcting the value of $N_{max}^{\ 0}$ from $5.14kB$ to $6.07k\pi a^2$.

- The differences between tension resistant and tension non-resistant soil materials combined with a tension non-resistant Tresca soil-foundation interface are important for small values of **n** and large values of **m,** *i.e.* for strongly eccentric loadings for which failure is governed by foundation uplift.. Otherwise, the values obtained for tension non-resistant materials are marginally smaller than the values obtained for tension resistant materials.

Interesting extensions of the proposed solution could deal with cohesionless materials, inhomogeneous soil properties (cohesion increasing linearly with depth), different geometrical configurations (embedment depth, rectangular footings).

7. ACKNOWLEDGEMENTS

The paper summarizes the current results obtained within the course of the doctoral thesis of the first author. This thesis is financially supported by Ecole Polytechnique (France) and the "Alexandros S. Onassis' Welfare Foundation (Greece). The authors are indebted to both organizations for their support.

8. NOTATIONS

Greek

γ= *Soil unit weight*
δ= *Geometrical parameter in mechanisms*
ε= *Geometrical parameter in mechanisms*
κ= *Geometrical parameter in mechanisms*
λ= *Geometrical parameter in mechanisms*
μ= *Geometrical parameter in mechanisms*
π= *Function of maximum resisting work*
ρ= *Soil mass density*
σ= *Normal component of stress on a plane*
$\underline{\underline{\boldsymbol{\sigma}}}$ = *Stress tensor*
Σ= *Surface of velocity discontinuity*
τ= *Tangential component of stress on a plane*
ω= *Angular velocity*
Ω= *Half – space of soil domain*

Latin

a= *Earthquake – induced soil acceleration*
a= *Radius of the foundation*
A= *foundation surface area*
B= *Strip foundation width*
c= *geometrical parameter in mechanisms*
$\underline{\underline{\mathbf{d}}}$ = *Strain rate tensor*
f_{soil}= *Yield function for soil medium*
f_{interf}= *Yield function for soil-foundation interface*
f_v= *Inertia soil force in the vertical direction*
f_h= *Inertia soil force in the horizontal direction*
$\mathbf{f_h}$= *Normalized horizontal inertial force*
FS= *Safety factor against bearing capacity failure*
k= *Soil and interface shear strength*
l= *Geometrical parameter in mechanisms*
M= *Resultant moment in the foundation*
m= *Normalized moment*
N= *Resultant vertical force in the foundation*
n= *Normalized vertical force*
$\underline{n}$ = *Unit normal vector*
Q_i= *Loading parameter of the system*
$\dot{q}_i$ = *Associated kinematic parameter for* Q_i
q= *Surcharge on the soil surface*
S_a= *Peak ground horizontal acceleration*
$\underline{\hat{U}}$ = *Virtual velocity vector*
$[\![\underline{\hat{U}}]\!]$= *Virtual velocity discontinuity*
V= *Resultant horizontal force on the foundation*
v= *Normalized horizontal force*

9. REFERENCES

Bransby, M. F., Randolph, M. F. (1998). "Combined loading of skirted foundations", *Geotechnique,* **48***, No. 5*, 637 - 655.

Cremer C., Pecker A., Davenne L. (2001). "Cyclic macro - element of soil - structure interaction: material and geometrical non-linearities", *International Journal of Analytical Methods in Geomechanics, vol.* **25**, 1257-1284.

Cremer C., Pecker A., Davenne L. (2002). "Modelling of non linear dynamic behaviour of a shallow foundation with macro - element", *Journal of Earthquake Engineering, Vol.* **6***, no. 2*, 175-212.

Green, A., P. (1954). "The plastic yielding of metal junctions due to combined shear and pressure", *Journal of Mechanics and Physics of Solids* **2** *(3)*, 197 - 211.

Gourvenec, S., Randolph, M. (2003). "Effect of strength non - homogeneity on the shape of failure envelopes for combined loading of strip and circular foundations on clay", *Geotechnique,* **53***, No. 6*, 575 - 585.

Mendoza, M. J., Auvinet, G. (1988). "The Mexico earthquake of September 19, 1985 - Behavior of building foundations in Mexico City", *Earthquake Spectra, Vol.* **4***, No. 4, 835 – 852.*

Paolucci, R., Pecker, A. (1997a). "Soil Inertia Effects on the Bearing Capacity of rectangular Foundations on cohesive Soils", *Engineering Structures, Vol.* **19***, No. 8,*, 637-643.

Paolucci, R., Pecker, A. (1997b). "Seismic Bearing Capacity of Shallow Strip Foundations on Dry Soils", *Soils and Foundations, Vol.* **37***, No. 3,*, 95-105.

Puzrin, A. M., Randolph, M. F. (2003a). "Generalized Framework for Three - Dimensional Upper bound Limit analysis in a Tresca Material", *ASME, Journal of Applied Mechanics, Vol.* **70** *(1)*, 91 - 100.

Puzrin, A. M., Randolph, M. F. (2003b). "New planar velocity fields for upper bound limit analysis", *International Journal of Solids and Structures,* **40***, No. 13 - 14*, 3603 - 3619.

Randolph, M. F., Puzrin, A. M. (2003). "Upper bound limit analysis of circular foundations on clay under general loading", *Geotechnique,* **53***, No. 9*, 785-796.

Salençon, J. (1974). "Bearing Capacity of a footing on a φ=0 soil with linearly varying shear strength", *Geotechnique,* **24***, No. 3*, p. 443 - 446.

Salençon, J. (1983). "Calcul à la rupture et analyse limite", *Presses de l'E.N.P.C., Paris*

Salençon, J. (1990). "An Introduction to the Yield Design Theory and its applications to soil mechanics", *European Journal of Mechanics, A/Solids,* **9***, No. 5*, 477-500.

Salençon, J., Matar, M. (1982). "Capacité portante des fondations superficielles circulaires", *Journal de*

Mécanique théorique et appliquée, Vol. **1***, No.* **2**,, 237 - 267.

Salençon, J., Pecker, A. (1995a). "Ultimate Bearing Capacity of shallow foundations under inclined and eccentric loads. Part I: Purely Cohesive Soil", *European Journal of Mechanics, A/Solids,* **14***, No. 3*, 349-375.

Salençon, J., Pecker, A. (1995b). "Ultimate Bearing Capacity of shallow foundations under inclined and eccentric loads. Part II: Purely Cohesive soil without tensile strength", *European Journal of Mechanics, A/Solids,* **14***, No. 3*, 377-396.

Salgado, R., Lyamin, A.V., Sloan, S.W., Yu, H.S. (2004). "Two- and three-dimensional bearing capacity of foundations in clay", *Geotechnique,* **54***, No.5*, 297-306.

Sekiguchi, H., Kobayashi, S. (1997). "Limit analysis of bearing capacity for a circular footing subjected to eccentric loadings", *Proceedings of the 14th ICSMFE, Hambourg Germany, 1997, Vol.* **2**, 1029 - 1032.

Taiebat, H. A., Carter, J. P. (2000). "Numerical studies of the bearing capacity of shallow foundations on cohesive soil subjected to combined loading", *Geotechnique,* **50***, No. 4*, 409 - 418.

Taiebat, H. A., Carter, J. P. (2002). "Technical Note. Bearing Capacity of strip and circular foundations on undrained clay subjected to eccentric loads", *Geotechnique,* **52***, No. 1*, 61-64.